Applied Energy 370 (2024) 123573

Contents lists available at ScienceDirect

Applied Energy

journal homepage: www.elsevier.com/locate/apenergy

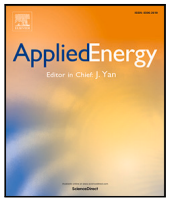

Probabilistic solar power forecasting: An economic and technical evaluation of an optimal market bidding strategy

L.R. Visser [a,*], T.A. AlSkaif [b], A. Khurram [c], J. Kleissl [c], W.G.H.J.M. van Sark [a]

[a] Copernicus Institute of Sustainable Development, Utrecht University, Utrecht, The Netherlands
[b] Information Technology Group, Wageningen University and Research, Wageningen, The Netherlands
[c] Center for Energy Research and Department of Mechanical and Aerospace Engineering, University of California, San Diego, CA, United States of America

ARTICLE INFO

Keywords:
Photovoltaic power
Probabilistic forecasting
Stochastic optimization
Electricity markets

ABSTRACT

Solar forecasting is a rapidly evolving field that can substantially contribute to the effective integration of large amounts of solar photovoltaic (PV) capacity into the electricity system. However, newly developed solar forecasting models are rarely tested in an operational context considering the intended application and objective. Besides, models are typically evaluated considering only technical error metrics, disregarding their economic value. This paper proposes an operational bidding strategy that optimizes the participation of a PV power plant in the electricity spot markets. To this end, a novel multistage stochastic optimization method is developed that considers the day-ahead, intraday, and imbalance markets. As the developed method utilizes a scenario generation algorithm, the proposed method can be adopted for a wide variety of related applications. The performance of the developed method is assessed using technical and economic metrics and compared to a reference method. The results demonstrate the effectiveness of the proposed bidding strategy, as it substantially outperforms the reference market bidding strategy. The findings also provide insights into the value of a multistage bidding method, as extending market participation from the day-ahead to the intraday market increases revenues by 22%, while halving the total imbalance. Additionally, the study examines the relationship between the technical and economic performance of solar power forecasting models, revealing a non-linear correlation.

1. Introduction

Supporting policies and rapidly decreasing costs triggered the exponential growth of solar photovoltaic (PV) systems since the turn of the century. By the end of 2022, over 1.1 TWp of PV capacity was installed [1], thus forming a substantial contribution to the power supply system in many countries across the globe. The increasing share of solar PV generation, and its intermittent and variable nature, affects the operation of the electricity system posing various technical challenges. These include power quality issues, such as voltage and frequency fluctuations, as well as challenges related to the balancing of supply and demand [2]. As the proliferation of PV is expected to continue in the coming decades, reaching up to 70 TWp by 2050 [3], these technical issues are foreseen to form a major hurdle for its successful integration. Hence, (additional) measures are needed to allow for cost-effective integration of vast amounts of solar PV in the electricity grid [4]. Reliable solar power forecasting models are widely identified as a key element to support the effective integration of large amounts of solar PV systems in the electricity grid [5,6]. Accurate forecasts can assist in the timely scheduling of the dispatch of power generators and batteries, and therewith ensuring grid stability, while reducing the need for balancing reserves. Amongst others, this would result in a reduced need for balancing capacity, thus limiting the cost of PV integration.

The interest in solar forecasting models increased significantly over the last decades [7]. In recent years attention shifted towards probabilistic models, which are preferred over point (or single-value) models as they provide information regarding the uncertainty of the forecast. Yet, recently Li and Zhang [8] pointed out a gap in literature regarding the development of probabilistic solar forecasting models and their application. Only a limited amount of studies are found that develop operational probabilistic solar power forecasting models that are applied to a specific problem, e.g. an energy management system [9], unit commitment problem [10] and day-ahead market (DAM) trading [11]. Therefore, Li and Zhang [8] suggested that more attention should be laid on the use of probabilistic forecasting models. Whereas probabilistic forecasts hold highly valuable information regarding the uncertainty of PV power generation, it does not account for the interdependencies between consecutive time-steps that capture the dynamics of the underlying system. This shortcoming could result in overlooking patterns that

* Corresponding author.
E-mail address: l.r.visser@uu.nl (L.R. Visser).

https://doi.org/10.1016/j.apenergy.2024.123573
Received 11 December 2023; Received in revised form 12 April 2024; Accepted 25 May 2024
Available online 8 June 2024

impact decision-making processes. Therefore, to address the identified gap in literature related to the application of probabilistic forecasts, it is crucial to develop methods that can convert probabilistic forecasts into scenarios.

Another unexposed theme in the field of solar forecasting concerns the unidimensional evaluation of the models. The performance of solar forecasting models is usually captured with technical error metrics, e.g., mean absolute error and root mean square error in case of point models or the Brier score and continuous rank probability score (CRPS) for probabilistic models [12]. As a result, the economic value of solar forecasting is commonly ignored. A couple of exemptions are found in literature, which explored the economic value of solar forecasting for standalone PV systems in various ways [13–17]. These studies assessed the value of one or multiple solar forecasting models in the DAM in five regions in the United States [13], California [14], Spain [15], Italy [16] and the Netherlands [17], respectively. In addition, these studies explicitly compared the relation between technical and economic metrics. Yet, these studies only consider point forecasting models and ignore probabilistic models. Bracalae et al. [18] evaluated the economic value of two Bayesian-based probabilistic forecasting models, using cost-based indices. The metric therefore allows to express the economic performance of (probabilistic) forecasting models by normalizing the economic value over the maximum value per time interval, much similar to, e.g., the weighted mean absolute error. However, since this study neglects the uncertainty in the defined bidding strategy, it ignores the potential of utilizing the additional value that is captured in probabilistic forecasts.

Besides, these studies [13–18] exclude the intraday market (IM), which can be used to correct for prediction errors that originate in DAM trading [19]. As a result, they overestimate the imbalance caused by trading electricity generated by PV systems in an operational setting and subsequently underestimate the value of solar forecasting [20–22]. In previous work, Silva et al. [21] identified the need for adequate bidding strategies that can deal with a multi-settlement framework (i.e. DAM and IM), while considering uncertainties, to facilitate the successful integration of variable renewable energy sources (VRES) in electricity markets and power systems. In literature, various studies are found that propose a wide variety of bidding strategies for wind power or wind combined with storage; an extensive overview is included in [23]. Others propose methods that output optimal bidding strategies for virtual power plants containing VRES and other assets that can potentially handle the uncertainties in the electricity generation by VRES including conventional thermal generators, storage and flexible loads, of which a comprehensive overview is given in [24]. In contrast, only few studies explore the development of market bidding strategies that are dedicated to PV systems. Although a variety of deterministic and stochastic market bidding strategies that consider a PV-battery system are proposed and applied to the DAM [25–27] or DAM and IM [28], none of these studies uses a solar forecasting model. Few other studies include a solar forecasting model in their proposed bidding strategy. For example, a bidding strategy for the DAM that considers stochastic optimization using an analog ensemble model to predict the PV generation is proposed in [29]. The study compares the results for a PV-battery system to a standalone PV system. Similarly, David et al. [30] compare several point solar forecasting models when used to optimize the DAM trading of a PV-battery system in Australia. Kakimoto et al. [11] developed a probabilistic solar irradiance forecasting model and used the forecasts for DAM trading in a case-study in Japan, providing insights in the technical accuracy and economic value. Yet, the developed method for market bidding relied on a simple linear model that described the relation between the solar irradiance and PV power output. Renkema et al. [31] developed several bidding strategies for PV power plant operators participating in the DAM, relying on solar PV forecasting models. This study considers forecast uncertainty using conformal prediction. Silva et al. [21] proposed a multistage stochastic optimization model for the optimal bidding of a virtual power plant composed of a wind plant, solar PV plant, and battery. The model considers the DAM and IM and relies on an artificial neural network to generate a set of scenarios. An overview of literature is presented in Table 1.

Overall, the current literature lacks studies that propose (probabilistic) solar power forecasting models and test their performance on the intended application. Moreover, probabilistic forecasts neglect the potential interdependencies between consecutive time-steps, what contains information that is paramount for many applications. As a result, there is a lack of studies that develop and evaluate operational stochastic bidding strategies for electricity markets that consider (standalone) PV systems and rely on (probabilistic) solar power forecasting models. In addition, these studies do not address the value of integrating IM trading alongside DAM trading, nor do they utilize state-of-the-art probabilistic solar power forecasting models. This paper aims to address these gaps by introducing a novel multistage stochastic optimization approach that generates bids for market participants operating a PV system. The main contributions of this paper can be summarized as follows:

1. The development of an operational multistage stochastic bidding strategy that considers the DAM, IM and balancing market, which can be used by PV system operators.
2. The application of a novel scenario generation algorithm that can transform time-independent probabilistic forecasts into interdependent scenarios.
3. The work exposes and quantifies the economic value of participating in the IM in addition to the DAM, and subsequently explores the relation between the lead-time and economic value of solar power forecasting models.
4. The work provides insight into the relationship between the economic value and technical accuracy of various point and probabilistic solar power forecasting models.

The performance of the proposed bidding strategy is tested and evaluated for three different probabilistic solar power forecasting models. The results are also compared to a reference bidding strategy, whose performance is tested considering four distinct point forecasting models.

The remainder of this paper is organized as follows. Section 2 discusses the methods and error metrics. Section 3 describes the data. Section 4 presents the results. The findings in this study are concluded in Section 6.

2. Methods

2.1. Stochastic bidding strategy

This study presents a novel multistage stochastic bidding strategy designed to optimize bidding strategies in electricity spot markets for a PV system, considering its inherent uncertainty of power generation. The bidding strategy first aims to maximize the expected value of participating in the DAM by placing an optimized bid ($\dot{p}_{\mathrm{DA}}$) for K forecast horizons, considering a set of Ω scenarios that is generated as explained in Section 2.4. The bid is generated by solving problem (1), as:

$$\underset{\dot{p}_{\mathrm{DA}}}{\text{maximize}} \quad \sum_{\omega=1}^{\Omega}\sum_{t=1}^{K}\Big(\lambda_{\mathrm{DA},t}\dot{p}_{\mathrm{DA},t} + b_t\lambda^{+}(p_{\omega,t}-\dot{p}_{\mathrm{DA},t}) - (1-b_t)\lambda^{-}(\dot{p}_{\mathrm{DA},t}-p_{\omega,t})\Big) \tag{1a}$$

$$\text{subject to} \quad 0 \le \dot{p}_{\mathrm{DA}} \le p_{\max}, \tag{1b}$$

where λ_{DA} is the (expected) DAM price. The DAM price is assumed to be known in this study, as these can be predicted with high accuracy [32]. The imbalance price $\lambda^{+/-}$ is defined as discussed in

Table 1
Overview of relevant literature. The table indicates the main characteristics of related work and amongst others indicate the focus of the evaluation being technical (tech) and/or economic (econ).

Reference	Assets or resources	Type of forecast	Type of model	Application	Evaluation	Operational	Bidding strategy
[11]	PV system	Forecast	Probabilistic	DAM	Tech and econ	No	Uncertainty considered
[13]	PV system	Forecast	Point	DAM	Tech and econ	No	–
[14]	PV system	Forecast	Point	DAM	Tech and econ	No	–
[15]	PV system	Forecast	Point	DAM	Tech and econ	Yes	–
[16]	PV system	Forecast	Point	DAM	Tech and econ	No	–
[17]	PV system	Forecast	Point	DAM	Tech and econ	Yes	–
[18]	PV system	Forecast	Probabilistic	–	Tech	No	Uncertainty not considered
[21]	VPP (solar, wind and battery)	Forecast	Point, set of scenarios	DAM and IM	Econ	Yes	Uncertainty considered
[25]	PV-battery system	Perfect foresight[a]	Point	DAM	Econ	No	–
[26]	PV-battery system	Perfect foresight[a]	Point	DAM and IM	Econ	No	–
[27]	PV-battery system	Perfect foresight[b]	Probabilistic	DAM	Tech	No	Uncertainty considered
[28]	PV-battery system	Perfect foresight[a]	Point	DAM and IM	Econ	No	–
[29]	PV & PV-battery system	Forecast	Probabilistic	DAM	Tech and econ	Yes	Uncertainty considered
[30]	PV-battery system	Forecast	Point	DAM	Tech and econ	Yes	–
[31]	PV system	Forecast	Point, conformal prediction	DAM	Tech and econ	Yes	Uncertainty considered

[a] Forecast introduced by adding an uncertainty (error) component to the PV power output.
[b] Probabilistic forecast introduced by adding an uncertainty (error) component to the PV power output and considering a distribution.

Section 2.5 and b_t is a binary variable expressed as:

$$b_t = \begin{cases} 0, & \text{if } \dot{p}_{\mathrm{DA},t} > p_{\omega,t} \\ 1, & \text{otherwise.} \end{cases} \tag{2}$$

The bid considers a set of scenarios as well as the potential economic consequences of a foreseen excess ($\dot{p}_{\mathrm{DA,t}} < p_{\omega,t}$) or shortage ($\dot{p}_{\mathrm{DA,t}} > p_{\omega,t}$) of power delivered to the grid in real-time. Furthermore, electricity can only be exported and the market bid is restricted by the grid capacity that is assumed to be equal to the nominal installed PV capacity ($p_{\max}$). Note that problem (1) results in a market bid expressed in power, whereas volume (energy) bids are placed in the market. Hence, the power bid is converted considering the temporal resolution (Δt), this also holds for the following problems.

Next, corrections to the initial DAM bid can be made in the IM, using updated PV power forecasts. The objective of this optimization problem is to maximize the expected value by bidding in the IM ($\dot{p}_{\mathrm{ID}}$) considering the updated forecasts as well as the initial bid to the DAM. Again, the consequences of deviations in real-time are considered by the imbalance prices for up- and down-regulation. An optimal ID bid is retrieved by solving problem (3), as:

$$\underset{\dot{p}_{\mathrm{ID}}}{\text{maximize}} \quad \sum_{\omega=1}^{\Omega}\sum_{t=1}^{K}\Big(\lambda_{\mathrm{ID},t}\dot{p}_{\mathrm{ID},t} + b_t\lambda^{+}(p_{\omega,t} - \dot{p}_{\mathrm{bid},t}) - (1-b_t)\lambda^{-}(\dot{p}_{\mathrm{bid},t} - p_{\omega,t})\Big) \tag{3a}$$

$$\text{subject to} \quad \dot{p}_{\mathrm{bid}} = \dot{p}_{\mathrm{DA}} + \dot{p}_{\mathrm{ID}}, \tag{3b}$$

$$0 \le \dot{p}_{\mathrm{bid}} \le p_{\max}, \tag{3c}$$

where λ_{ID} is the IM price.

2.2. Reference bidding strategy

In the reference bidding strategy market bids are based on point solar power forecasts. Since these point forecasts do not provide any information regarding the uncertainty of the prediction, the potential monetary impact of an imbalance is not considered. Therefore, the DA reference bidding strategy can be viewed as a simplified version of problem (1), where the bid is generated by solving problem (4), as:

$$\underset{\dot{p}_{\mathrm{DA}}}{\text{maximize}} \quad \sum_{t=1}^{K}\Big(\lambda_{\mathrm{DA},t}\dot{p}_{\mathrm{DA},t}\Big) \tag{4a}$$

$$\text{subject to} \quad \dot{p}_{\mathrm{DA},t} = \hat{p}_t - p_{\mathrm{curt},t}, \tag{4b}$$

$$0 \le \dot{p}_{\mathrm{DA},t} \le \hat{p}_t, \tag{4c}$$

where $\hat{p}$ presents the forecasted power output of a PV system and p_{curt} is the curtailed power. In contrast to (1), this variable is made explicit in condition (4b) to prevent bids that exceed the forecasted value while allowing for $\dot{p}_t = 0$. In practice, the reference bidding strategy generates a bid that is equal to the point forecast except when negative market price occurs. In the latter case, the market bid is set to 0.

Similarly, IM bids are generated by solving problem (5), as:

$$\underset{\dot{p}_{\mathrm{ID}}}{\text{maximize}} \quad \sum_{t=1}^{K}\Big(\lambda_{\mathrm{ID},t}\dot{p}_{\mathrm{ID},t}\Big) \tag{5a}$$

$$\text{subject to} \quad \dot{p}_{\mathrm{ID},t} = \hat{p}_t - \dot{p}_{\mathrm{DA},t} - p_{\mathrm{curt},t}, \tag{5b}$$

$$\dot{p}_{\mathrm{bid}} = \dot{p}_{\mathrm{DA}} + \dot{p}_{\mathrm{ID}}, \tag{5c}$$

$$0 \le \dot{p}_{\mathrm{bid},t} \le \hat{p}_t. \tag{5d}$$

2.3. Solar forecasting models

In this study, both point and probabilistic models are employed to forecast the PV power generation. The point forecasting models include a multi-variate linear regression (MLR), random forest regression (RF), physical PV and a smart (clear sky) persistence (SP) model. The MLR model assumes a linear relationship between predictor variables and the target variable (PV power output). In this study, the MLR model uses the least squares loss function to determine the coefficients. The RF model is a nonlinear model that consists of a predefined number of trees, each made up of t layers and 2^t decision nodes. The trees are built independently by considering bootstrap samples of the training data. Next, random subsets are selected to construct the decision nodes within each tree, a process that relies on a loss function. Here, the least squares loss function is considered. The predicted value, i.e. output, of the RF model is presented by the conditional mean of all constructed trees. The PV model predicts future PV generation values by considering a chain of physical models/equations, namely a decomposition, transposition and a PV simulation model. Last, the SP model generates forecasts by deriving clear sky indices from the last PV power output recordings, concerning the expected power output for clear sky conditions. The indices are then extrapolated to future timestamps.

The probabilistic models considered are quantile regression (QR), quantile regression forest (QF) and clear sky persistence ensemble (CSPE). In the QR model, a linear relationship between predictor and target variables is established, with coefficients independently learned for each percentile. These are estimated by minimizing the sum of absolute residuals over the asymmetrically applied weights error. The QF model operates similarly to the RF model, with the mean value per node replaced by the distribution of observations. The output of the QF model thus provides a conditional distribution function. For both

the QR and QF models, a 99% prediction interval is considered, using a total of 21 quantiles covering an interval from 5% to 95%, and a lower and upper bound of 0.5 to 99.5%. The CSPE model considers the last 21 recordings, collectively forming a distribution. All forecasting models presented here are discussed in more detail in [33].

Although the aforementioned models are used for both DA and ID forecasting, the input information they take into account varies. The DA forecasting models consider the same predictor variables as discussed in [33]. These include various irradiance components, wind speed, temperature, cloud cover and pressure. In addition to these variables, the ID models also incorporate lagged power generation values observed over the previous 3 h.

In addition to being either point and probabilistic models, these models can be classified according to the input information they rely on. The SP, MLR, RF, QR and QF receive new information at each forecast issue time. The CSPE model is only updated at midnight, whereas the physical PV model is updated following the issue of numerical weather predictions (NWPs) at midnight and noon.

2.4. Scenario generation

The interdependence structure of forecast errors on sequential time horizons is essential to support time-dependent decision making, like multi-market participation with a PV-battery system. Yet, probabilistic forecasts neglect this interdependence structure. Pinson et al. [34] proposed a statistical method that can transform probabilistic forecasts to scenarios that consider the interdependence structure of the prediction errors. The method was originally developed for the purpose of wind power forecasting and was later also successfully used for net load forecasting, i.e. demand subtracted with solar generation [35]. In this study, the method is adopted for the purpose of building scenarios from probabilistic PV power forecasts. As a first step a random variable Y_k is generated from the probabilistic forecasts ($\hat{F}_{t+k|t}$), using the probability integral transform (PIT):

$$y_{k,t} = \hat{F}_{t+k|t}(\hat{p}_{t+k}),\ \forall t \tag{6}$$

where $\hat{F}_{t+k|t}$ denotes the cumulative distribution function (CDF) of the probabilistic forecasts $\hat{f}_{t+k|k}$ at time t with horizon k. Given that the generated probabilistic forecasts are in a discrete form, it is necessary to convert them into a continuous CDF to facilitate the PIT. To achieve this, a smooth curve is fitted to the set of predicted quantiles.

A key assumption of the scenario generation method is for the probabilistic forecasts to be reliable, which implies that a sample from the predictive CDF should be statistically similar to the observations. This is true if Y_k is uniformly distributed on the unit interval, i.e. $Y_k \sim \mathrm{U}[0,1]$.

Next, the probit function (Φ^{-1}) i.e. inverse of the Gaussian CDF can be applied to transform Y_k to a normally distributed random variable X_k with zero mean and unit standard deviation, i.e. $X_k \sim \mathrm{N}(0,1)$:

$$x_{k,t} = \Phi^{-1}(y_{k,t}),\ \forall t. \tag{7}$$

Considering the transformed random variable X_k for each horizon k ($k = t_0, \ldots, K-1$), a random vector $\mathbf{X} = (X_1, \ldots, X_{K-1})^\intercal$ can be constructed. The assumption is made that $\mathbf{X}$ follows a multivariate Gaussian distribution, denoted as $\mathbf{X} \sim N(\mu_0, \mathbf{\Sigma})$, where μ_0 is a vector of zeros and Σ represents the covariance matrix capturing the temporal dependency between the forecast horizons of interest, $k = t_0, \ldots, K-1$. An unbiased estimation of the matrix $\mathbf{\Sigma}$ can be obtained by:

$$\mathbf{\Sigma_t} = \frac{1}{t-1}\sum_{j=1}^{t} \mathbf{X}_j \mathbf{X}_j^\intercal. \tag{8}$$

The temporal dependence captured in the covariance matrix is anticipated to change over time, and particularly in different seasons characterized by distinct prevailing weather patterns. The covariance matrix $\mathbf{\Sigma}$ that considers a subset of historical samples is therefore updated for each time-step. In an iterative process, the size of the subset was empirically set to 30 days.

By employing a multivariate Gaussian random number generator with parameters μ_0 and $\mathbf{\Sigma}$, a set of Ω scenarios is generated. These scenarios represent Ω realizations of the random vector $\mathbf{X}$. Subsequently, Ω realizations of $\mathbf{Y_k}$ can be constructed using the CDF (Φ):

$$y_{\omega,k} = \Phi(x_{\omega,k})\ \forall \omega, k. \tag{9}$$

As a last step, the forecast scenarios are generated with:

$$\hat{p}_{\omega,t+k|t} = \hat{F}^{-1}_{t+k|t}(y_{\omega,k}),\ \forall \omega, k. \tag{10}$$

Fig. 1 presents an example of the results for the presented scenario generation algorithm for a DA (Fig. 1a and b) and ID forecast (Fig. 1c and d). Fig. 1a and c present the predictive distributions of the PV power output. The updated (ID) forecasts in Fig. 1c result in a sharper predictive distribution. This is especially observed in the first hours following the forecast issue time, which is exemplary for shorter forecast horizons. Note the different time resolution used in the models, where the maximum expected PV power output increases in case of the ID forecast as a result of reduced temporal smoothing.

Last, while the incorporation of the scenario generation algorithm within the bidding approach presents numerous benefits, it is noteworthy that in the specific application under investigation (e.g. standalone PV system) scenarios could alternatively be represented using probabilistic quantiles.

2.5. Imbalance scenarios

Two different scenarios for imbalance penalization are considered. The first strategy assumes a static imbalance penalty, which is considered as a benchmark scenario:

$$\lambda^+ = c_1 \tag{11}$$

$$\lambda^- = c_2, \tag{12}$$

where c_1 and c_2 present constants, which are varied as part of a sensitivity analysis to obtain the optimal value (See Section 4.5). In the second (main) strategy the imbalance penalty depends on the electricity price and therefore varies over time. This dynamic imbalance penalty scenario is expressed as:

$$\lambda^+ = \lambda_{\mathrm{DA},t} + c_1 \tag{13}$$

$$\lambda^- = \lambda_{\mathrm{DA},t} + c_2. \tag{14}$$

2.6. Operational aspects of the bidding strategy

The operational aspects of the bidding strategy are defined by the market constraints and set the requirements to the solar forecasting models. Table 2 presents a summary of the DAM and IM characteristics in the Netherlands, which define the lead-time, time horizon, temporal resolution and update rate.

Table 2
Day-ahead and intraday spot market (DAM and IM) characteristics in the Netherlands.

	DAM	IM
Gate closure time	12:00 at D	Continuous
Lead-time[a]	12 h	5 min
Horizon[a]	12–36 h	5 min to end of $D+1$
Resolution	Hourly	15 min
Update rate	Daily	Continuous
Type	Market clearing price	Pay-as-bid

[a] These values present the actual lead-time and horizon and do not account for the issue time associated with e.g. the NWP variables (see Section 3.2).

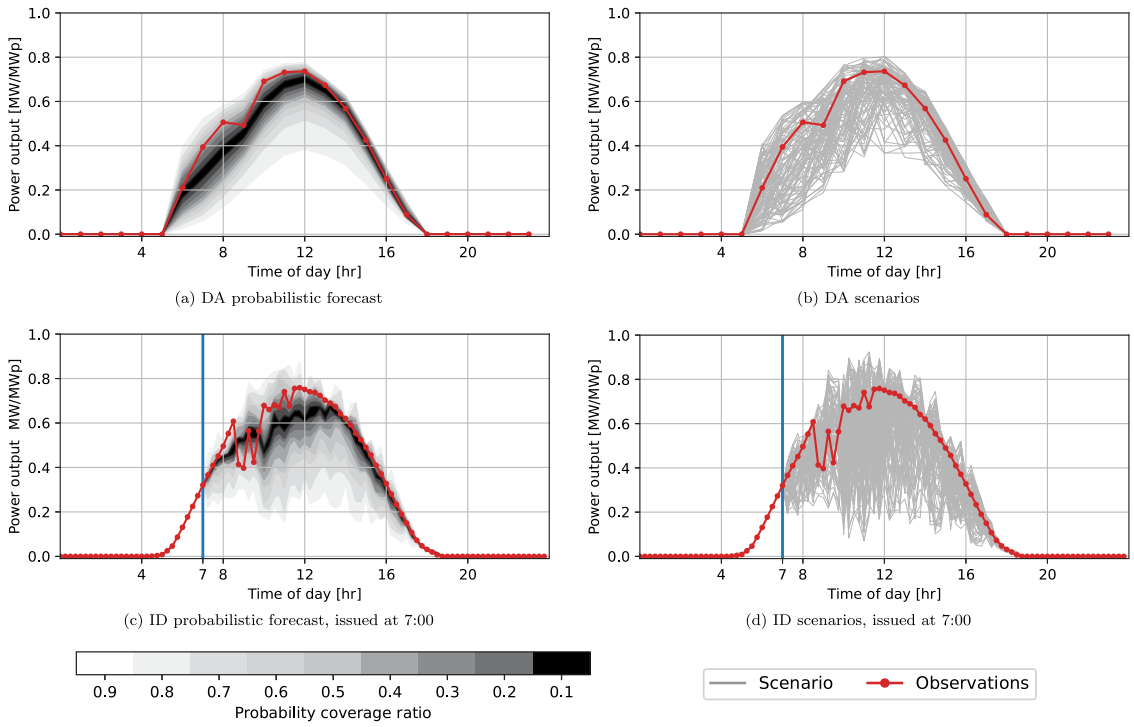

Fig. 1. Example of the DA (a,b) and ID (c,d) probabilistic forecasts and subsequent 100 scenarios of the expected PV power output for April 26, 2020. The blue vertical line in Fig. 1c and d presents the forecast issue time, i.e. 7: 00.

2.7. Tools for evaluation

2.7.1. Solar forecasting models

The technical performance of the forecasting models are in this study primarily evaluated considering the continuous ranked probability score (CRPS). The CRPS is a numerical error metric that captures both the reliability and sharpness of probabilistic models. The CRPS can also be applied to assess the performance of point models, where the value is comparable to the mean absolute error [36]. The CRPS rewards a high concentration of the forecasted probability around the target value. The CRPS is expressed as:

$$CRPS = \frac{1}{T}\sum_{t=1}^{T}\int_{-\infty}^{\infty}(F_t(x) - \hat{F}_t(x))^2 dx, \tag{15}$$

where $F_t(x)$ and $\hat{F}_t(x)$ are the CDFs of the observations and forecasts at time-step t in T. In (15) $F_t(x)$ presents a cumulative-probability step function as it describes a point that jumps from 0 to 1 at the observed PV power generation [12]. Similarly, in case of a point forecast $F_t(x)$ presents a step function. Nighttime values defined as $p_t = 0$ are removed before evaluation.

2.7.2. Solar scenarios

The PV power generation scenarios are evaluated in two steps. First, the calibration of the probabilistic forecasting models and the assumption of a uniform distribution are assessed using a PIT histogram. A uniform distribution indicates that the forecast probabilities are well calibrated with the actual observations. The histograms are evaluated separately for each forecast horizon, considering consistency bars that present a lower and upper bound to account for randomness as suggested in [37].

Second, the scenarios are evaluated using two prerank functions: the average rank and band depth rank histogram (ARH and BDH), as set forth in [35] and originally proposed in [38]. These prerank functions provide insights in the calibration of scenarios and their interdependence structure. In particular, the ARH provides insights in the distribution of multivariate scenarios similarly to the PIT histogram does for univariate ensemble members, whereas the BDH assesses the correlation. The objective of a prerank function is to rank the trajectories of the generated scenarios and observation vector. The results can be visualized in a rank histogram, which quantifies the frequency of observations that fall between two ensemble members. The rank histogram is evaluated similarly to a PIT histogram, where a uniform distribution of the rank histogram indicates well calibrated multivariate scenarios. To this end, the scenarios ($\mathbf{p}_\omega$) and observation vector ($\mathbf{p}$) are collected in a matrix B with dimensions $K \times J$, where $J = S + 1$. The rank histograms are then calculated following three main steps. First, univariate preranks are assigned to the ensemble members and observations with:

$$c_k(\mathbf{p}_\omega) = \sum_{j=1}^{J}\mathbf{1}\{p_{j,k} \le p_{\omega,k}\}, k = 1, \dots, K. \tag{16}$$

where $\mathbf{1}$ denotes an indicator function and c_k presents the prerank for each k-ensemble member or observation. As a second step, the multivariate preranks can be calculated and assigned to the scenarios and observation vector using the prerank functions π_B^{ARH} and π_B^{BDH}, respectively:

$$\pi_B^{ARH}(\mathbf{p}_\omega) = \frac{1}{K}\sum_{k=1}^{K} c_k(\mathbf{p}_\omega), \tag{17}$$

$$\pi_B^{BDH}(\mathbf{p}_\omega) = \frac{1}{K}\sum_{k=1}^{K}(J - c_k(\mathbf{p}_\omega))(c_k(\mathbf{p}_\omega) - 1). \tag{18}$$

As a third step, the rank histogram bin (b) of the observation vector is found per prerank function within the collection of preranks presented in B with:

$$b = 1 + \sum_{s=1}^{S}\mathbf{1}\{\pi(\mathbf{p}_s) < \pi(\mathbf{p})\}. \tag{19}$$

The reader is referred to [38] for a complete discussion on the interpretation of the rank histograms.

2.7.3. Market participation

The economic performance of the forecasting models is measured considering the economic revenue (ER), which is calculated as:

$$ER = \lambda \dot{p}_{\text{bid}} + \begin{cases} \lambda^{+}(p - \dot{p}_{\text{bid}}) \text{ if } y > \dot{p}_{\text{bid}} \\ \lambda^{-}(p - \dot{p}_{\text{bid}}) \text{ if } y \leq \dot{p}_{\text{bid}} \end{cases} \quad (20)$$

where p is the PV power generation and $\dot{p}$ is the optimized bid to the electricity spot market. The value of λ^{+} and λ^{-} are set by the transmission system operator (TSO) and depend on the state of the electricity system at time t. In practice surpluses are most often compensated, whereas deficits are penalized, but exemptions occur. Since for most of the time λ exceeds λ^{+}, trading energy in the spot markets is most profitable. Similarly, as λ^{-} is typically higher than λ, the costs of shortages exceed the initial profits made in the electricity spot markets.

3. Data collection

3.1. PV power generation

The PV power generation data is acquired by simulating the power output of a 1 MWp PV system, using a PV model from *pvlib* [39]. The steps required to simulate the PV power output are discussed in Section 2.2.1 of [33]. The model requires the input of the measured global horizontal irradiance (GHI), ambient and dew point temperature, wind speed and surface pressure, which are collected from the weather station in Cabauw, the Netherlands (51°97′N, 4°926′E) [40]. The measurements feature a 10 min resolution; 15 min and hourly values are obtained through resampling. In this study, data from 2018 to 2020 is considered, where 2018 and 2019 are used for training and validation purposes and 2020 concerns the test period.

3.2. Weather forecasts

Weather forecasts are for the same period obtained from the European Centre for Medium-Range Weather Forecasts (ECMWF) [41]. The weather forecasts are acquired from the 0: 00 and 12: 00 UTC model runs generated by the high resolution forecast configuration (HRES) of the Integrated Forecast System (IFS), which is a NWP system. Given that these forecasts by ECMWF are dispatched approximately 6 h after the commencement of the run, an additional forecast lead-time of 6 h is considered regarding the availability of these predictions. The distributed forecasts feature a spatial resolution of approximately 9 km, specific values are obtained using spatial interpolation [41]. The collected variables include the ambient and dew point temperature, GHI, total cloud cover, zonal and meridonal wind speed and total precipitation. Additional predictor variables are created following the three post-processing steps discussed in [33]. As the forecasts are published with an hourly resolution, 15 min values are obtained by means of linear interpolation for all variables except GHI. The 15 min GHI values are found through linear interpolation of the clear sky index.

3.3. Electricity prices

Electricity spot market prices are collected from the ENTSO-E transparency platform [42]. As only DAM prices are publicly available, IM prices are assumed to be identical. This assumption is substantiated as average IM prices are very similar to and strongly correlate with DAM prices [43]. Yet, actual IM prices can still differ from DAM prices, possibly altering the results. This impact is however expected to be negligible as it will likely have a similar effect on all models. The imbalance prices are acquired from TenneT, the TSO in the Netherlands [44]. Fig. 2 presents the distribution of DAM and imbalance prices as well as the average values.

Table 3
Summary statistics of the transformed random variables X_k. The statistics present the mean (μ), standard deviation (σ), skewness (γ) and excess kurtosis (κ), expressed by the mean and standard deviation over all forecast horizons.

Model	$\bar{\mu}_X \pm \sigma(\mu_X)$	$\bar{\sigma}_X \pm \sigma(\sigma_X)$	$\bar{\gamma}_X \pm \sigma(\gamma_X)$	$\bar{\kappa}_X \pm \sigma(\kappa_X)$
QR	-0.012 ± 0.02	0.96 ± 0.01	-0.027 ± 0.02	-0.22 ± 0.16
QF	0.023 ± 0.03	0.94 ± 0.02	-0.038 ± 0.02	-0.19 ± 0.12

4. Results

4.1. Scenario generation

The scenario generation approach followed in this study (see Section 2.4) assumes the probabilistic forecasts to be uniformly distributed $U[0, 1]$ in order to transform the predictions to a normal distribution $N(0, 1)$. Fig. 3 shows the validity of the assumption by presenting the PIT diagrams of the QR model. Although some outliers are found in the columns on the left, overall the results show that the assumption holds as the majority of the bars remain within the margins of the consistency bars presented by the dotted blue lines. The PIT diagrams in Fig. 3b, c and d indicate a general trend where the quantiles around the median are slightly under-represented, such that the surrounding quantiles are lightly over-represented. This trend was observed for all forecast horizons that exceed 1 h. Similar results were found for the QF model.

The right column in Fig. 3 presents the histogram of the random variable X_k for the same forecast horizons. Additionally, similar to Table 1 in [34] and Table 2 in [35], Table 3 summarizes the statistical characteristics of the distribution of X for both the QR and QF model, for all forecast horizons. The table shows the mean ($\bar{.}$) and standard deviation ($\sigma(.)$) of the mean (μ), standard deviation (μ), skewness (γ) and excess kurtosis (κ). The results obtained for the first four moments are similar to the results found in [34,35]. Remarkable, however, is that in contrast to these studies, the results show a negative excess kurtosis implying that the distribution of X is flatter featuring slightly shorter tails compared to a standard normal distribution $N(0, 1)$, i.e. less outliers are observed. Although the excess kurtosis values are low, this indicates that the predicted distributions could be sharper, which is in line with the results observed in the PIT-diagram visualized on in Fig. 3. Overall, considering the first four moments, the distribution of X over all horizons ($\mathcal{K}$) is on average approximately similar to a standard normal distribution of $N(0, 1)$.

Fig. 4 shows the ARH and BDH results for a single forecast issue time at noon for the next day (DA forecast) of the QR model. As the histograms show a flat distribution, the obtained results are considered satisfactory. Similar results are found for the other forecast issue times as well as the QF model.

4.2. DA and ID forecasts

The numerical technical results of the PV power forecasting models are summarized in Table 4. The values present average values over all forecast horizons $\mathcal{K}$. For the ID and DA forecasts these concern 0–24 h and 12–36 h ahead, respectively. Note that the DA and ID forecast models cannot be compared directly, as the DA models consider an hourly resolution, where the ID models feature a quarterly resolution. For the QR and QF models, Table 4 also presents the obtained CRPS values considering the generated scenarios. For this purpose, the CRPS is calculated by considering the scenarios as an equally spaced probabilistic forecast, i.e. since 100 scenarios ($\Omega = 100$) are considered each scenario is assumed to present a 1% quantile. A few general conclusions can be drawn considering the DA and ID forecasts. First, Table 4 clearly shows that the probabilistic forecasting models (QR and QF) outperform the point models. Second, the results demonstrate the dominance of tree-based models, where the RF and QF models outperform all

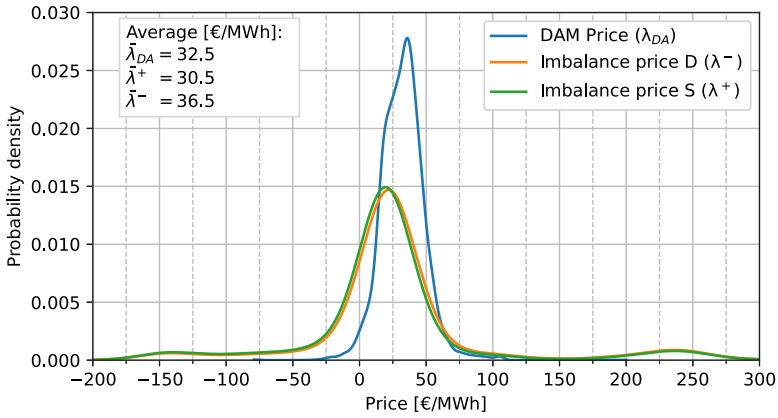

Fig. 2. Distribution of the DAM price and imbalance prices in case of a production deficit (D) or surplus (S) for daytime values in 2020, i.e. times where a (positive) power output of PV systems was registered. The subfigure presents the average DAM and imbalance prices.

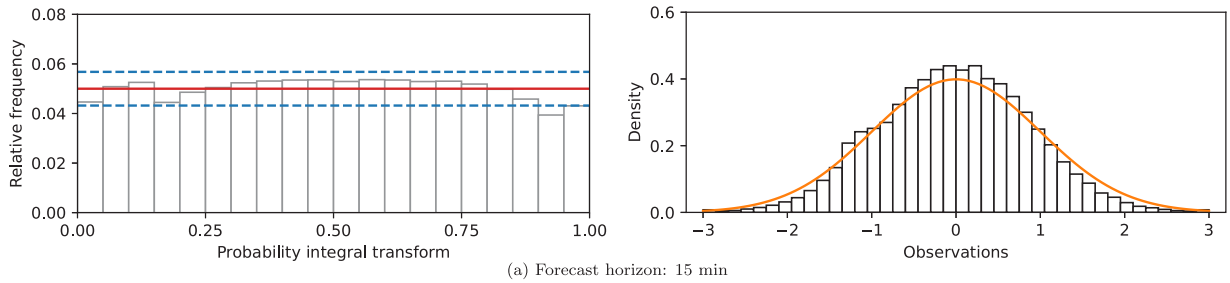

(a) Forecast horizon: 15 min

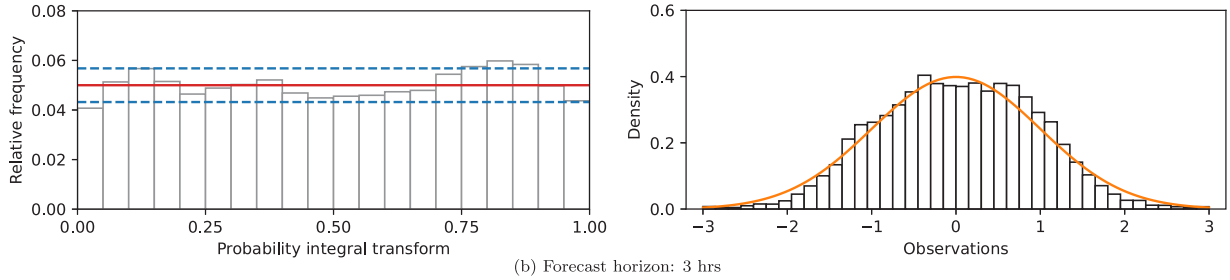

(b) Forecast horizon: 3 hrs

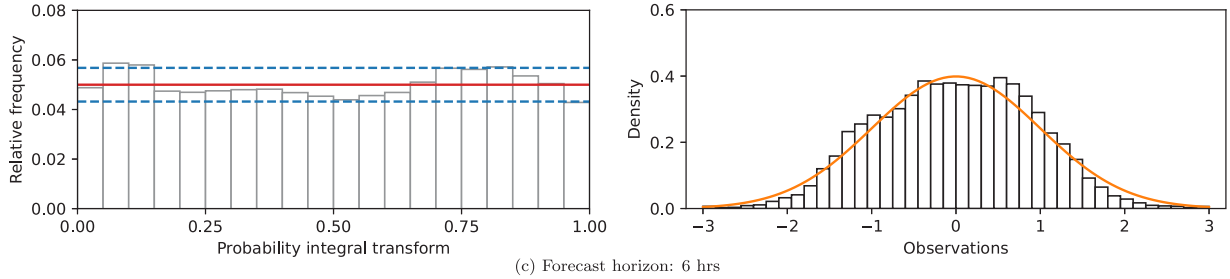

(c) Forecast horizon: 6 hrs

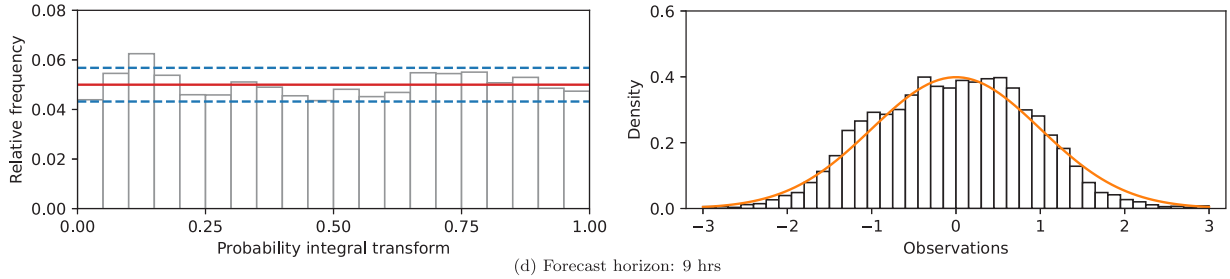

(d) Forecast horizon: 9 hrs

Fig. 3. The probability integral transform (Y_k) on the left and observed transformed random variable (X_k) on the right for four distinct forecast horizons of the QR model. The red line presents a perfectly calibrated forecast for U[0,1], the blue dotted lines indicate the consistency bars. The orange line presents the probability density function of a normal distribution N(0,1). Similar results are found for the QF model.

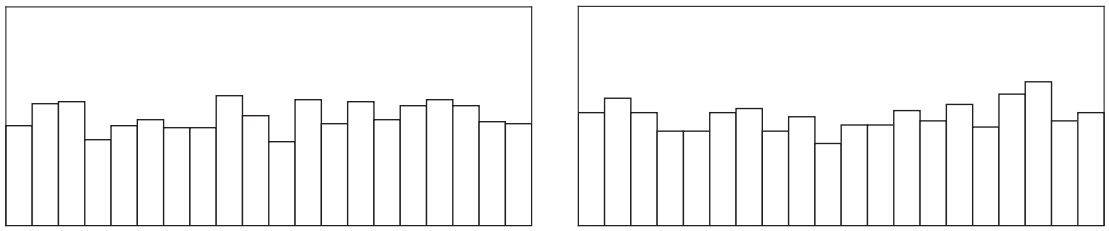

(a) ARH (b) BDH

Fig. 4. Average rank histogram (ARH) and band depth histogram (BDH) for a single forecast issue time, i.e. 12:00 at D. Similar results are found for other forecast issue times.

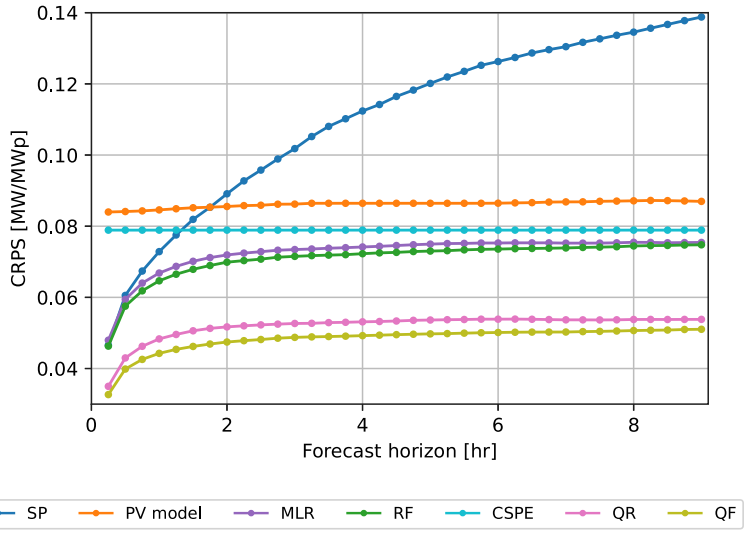

Fig. 5. The average CRPS of the ID point and probabilistic forecasting models per forecast horizon.

other DA and ID point and probabilistic models, respectively. Yet, the differences in the CRPS are much more significant for DA forecasts compared to ID forecasts. Furthermore, the accuracy obtained for the generated scenarios are similar to the probabilistic models from which they originate.

Fig. 5 shows the CRPS of the ID forecasting models per forecast horizon. As expected the accuracy of the models is highly affected by the horizon. In general, the results in Fig. 5 indicate that the CRPS deteriorates with an increasing time horizon, especially within the first hour. In short, this is explained by the temporal correlation of the PV power output. The lagged generation values form the most important predictor variables for predictions that feature a forecast horizon of up to 1 h ahead. Model simulations show that as the forecast horizon increases, the NWP variables gain importance and these predictor variables surpass the importance of the lagged values from forecast horizons that exceed 1 h ahead. This observation is exemplified by the disconnection of the CRPS trajectory of the SP model compared to the other point models MLR and RF. The performance of the SP model deteriorates more rapidly and significantly compared to the MLR and RF models, as it only considers the PV power output that is available at the forecast issue time and excludes the NWP variables. Since the NWP variables are only updated twice per day, the accuracy of the ID forecasting models stabilizes from the point that these variables predominate. This also explains the PV model's consistent performance over time. In case more NWP runs would be available, improved model accuracy is expected especially for shorter forecast horizons.

Furthermore, Fig. 5 shows that tree-based models (RF and QF) dominate by outperforming other point and probabilistic models, respectively, for all forecast horizons.

Table 4
The CRPS per DA and ID PV power forecast model over all realizations of $\mathcal{K}$ forecast horizons.

Model	CRPS (DA)		CRPS (ID)	
	Original	Scenario	Original	Scenario
SP	11.1		11.0	
PV	9.5		8.9	
MLR	8.2		7.4	
RF	7.0		7.2	
CSPE	7.9		7.9	
QR	6.1	5.7	5.3	5.2
QF	**4.8**	**4.8**	**4.9**	**4.8**

4.3. Market trading

The technical and economic results of participation in spot markets are, for various forecast horizons, summarized in Table 5 and depicted in Fig. 6. Since the results for $k > 3$ h ahead are very similar to $k = 3$, these are excluded from Table 5. Note that in case of IM trading, the DAM trades are followed by IM trades considering the specified horizon. The results are compared to market participation in case of perfect solar forecasting, i.e. considering PV power measurements (red horizontal bar in Fig. 6). The results in Table 5 show an improved performance of market participation, in terms of the imbalance caused and revenues generated, when DAM trades are supplemented with IM trades. In general, the results show a trend in improved performance as the forecast horizon reduces with higher marginal gains related to IM trading. Hence, most value lies within the final moments prior to delivery and therefore last minute trading is preferred from a perspective of the PV plant operator. This observation holds for all models

Table 5
Numerical results of market participation per forecast model for several forecast horizons (k). The results for ID trading combine DA trades with one-off ID trades at the specified time horizon. The results of $k = 6$ and $k = 9$ are similar to $k = 3$. The technical column presents the quantitative results of trading energy. The economic column shows the net monetary results of market participation. DA presents the results for all energy traded in the DAM, whereas ID is the absolute sum of trades in the IM. IMB presents the total imbalance caused, i.e. absolute sum of the surplus (S) and deficit (D).

Model	Technical [MWh/MWp]					Economic [€/MWp]				
	DA	ID	S	D	IMB	DA	ID	S	D	Total
Perfect forecasting (PF)										
PF	1051					27 080				27 080
Forecast horizon: 15 min										
SP	1024	571	**96**	−116	212	28 236	−306	2177	−3197	26 910
PV	981	255	202	−166	368	26 932	−450	3321	−7016	22 786
MLR	1003	360	104	−103	206	27 985	−435	1987	−3685	25 852
RF	1004	312	100	−99	199	27 712	−88	1686	−3489	25 820
CSPE	1080	236	250	−273	523	30 109	−1454	3227	−13 562	18 321
QR	928	423	101	−98	199	25 179	2219	2347	−2778	**26 967**
QF	959	346	100	**−97**	**197**	25 717	1722	2155	−2882	26 712
Forecast horizon: 1 h										
SP	1024	577	148	−203	352	28 236	949	3133	−6557	**25 760**
PV	981	250	203	−169	372	26 932	−362	3283	−7236	22 617
MLR	1003	310	147	−143	290	27 985	−478	2498	−6072	23 932
RF	1004	254	**141**	−137	278	27 712	−141	2144	−5883	23 831
CSPE	1080	236	250	−273	523	30 109	−1454	3227	−13 562	18 321
QR	928	373	151	−132	283	25 179	1597	3037	−4693	25 120
QF	959	302	143	**−127**	**270**	25 717	1161	2687	−4714	24 850
Forecast horizon: 2 h										
SP	1024	572	182	−268	450	28 236	2142	2946	−9954	23 370
PV	981	250	203	−169	372	26 932	−362	3283	−7236	22 617
MLR	1003	296	161	−152	313	27 985	−646	2468	−6873	22 934
RF	1004	235	**155**	−145	300	27 712	−357	2116	−6627	22 844
CSPE	1080	236	250	−273	523	30 109	−1454	3227	−13 562	18 321
QR	928	351	166	−141	307	25 179	1315	2897	−5603	**23 788**
QF	959	287	158	**−132**	**280**	25 717	681	2616	−5278	23 736
Forecast horizon: 3 h										
SP	1024	542	206	−311	520	28 236	2963	2928	−12 436	21 691
PV	981	250	203	−169	372	26 932	−362	3283	−7236	22 617
MLR	1003	288	165	−154	319	27 985	−699	2422	−7092	22 616
RF	1004	232	**161**	−146	307	27 712	−468	2136	−6831	22 549
CSPE	1080	236	250	−273	523	30 109	−1454	3227	−13 562	18 321
QR	928	348	170	−143	313	25 179	1294	2816	−5779	23 510
QF	959	285	163	**−135**	**297**	25 717	730	2626	−5496	**23 576**
Forecast horizon: 12–36 h										
SP	1024		296	−278	574	28 236		2097	−13 250	17 083
PV	981		247	−214	461	26 932		3802	−10 138	20 596
MLR	1003		217	−206	423	27 985		2371	−10 378	19 978
RF	1004		**192**	−183	375	27 712		1783	−9772	19 723
CSPE	1080		276	−314	590	30 109		2401	−14 140	18 370
QR	928		252	**−156**	408	25 179		3701	−7157	21 723
QF	959		213	−157	**370**	25 717		3147	−6817	**22 047**

that receive updated information at each forecast issue (SP, MLR, RF, QR and QF). Furthermore, considering the best performing model per forecast horizon, revenues increase with 22.3% from 22.0 k€/MWp to 27.0 k€/MWp per year when DAM trades are updated with IM trades. As a result, the economic revenues are almost equal to the revenues in case of perfect forecasting. Similarly, the imbalance caused almost halves (−46.8%). Note that in practice the revenues that can be generated from participation in the IM also depend on the market's liquidity.

Overall, the probabilistic models exhibit superior performance compared to the other models across the majority of time horizons in terms of generating the highest revenues and minimizing imbalances (see Table 5). Only SP demonstrates competitive results for $k = 1$ and $k = 4$. Among the considered horizons, QF produces the lowest imbalance, while QR achieves the highest revenues for most instances.

4.4. Trading revenues to forecast accuracy

Although from Table 5 it appears that improved model accuracy's (lower imbalances) lead to higher revenues, closer inspection of the results show that the imbalance and revenues are not linearly related. Exemplary for this is the relatively high imbalance caused by SP for $k = 4$, while it earns the highest revenues. This relation is further explored in Fig. 6, which explicitly plots the revenues to the CRPS. First focusing on Fig. 6(b), it can be observed that improved model accuracy does not lead to higher revenues. For example, the RF model obtains a significantly lower CRPS compared to MLR and SP, but yields lower market trading revenues. In short, this is explained by the state of the electricity system being either short or long at the time an imbalance occurs.

Yet, focusing on a specific model, e.g. MLR, it can be noticed that the generated revenues increase with improved accuracy, resulting from reduced forecast horizons. This observation is supported by Fig. 6(a), which indicates an approximate linear relation between the accuracy and economic revenue per forecast model; this trend is observed for MLR, RF, QR, QF or SP.

4.5. Imbalance penalty sensitivity analysis

Both a static and dynamic strategy are considered for setting the imbalance penalty as part of the stochastic bidding strategy, see problem (1) and (3). Fig. 7 presents the results for these two strategies for $k = 1$, while considering the QR model. Similar trends are found for the other forecast horizons as well as the QF model. Fig. 7 clearly shows that adopting the dynamic strategy results in higher economic revenues. For this scenario, a higher economic revenue is obtained when $|\lambda^+| \approx |\lambda^-|$, i.e. the imbalance penalty in case of a surplus or deficit is in balance, which is the case when $|c_1|$ is approximately equal to $|c_2|$. The single most optimal value i.e. highest economic value is indicated by the red dot. This is also the imbalance scenario considered in the results presented in Sections 4.3 and 4.4. The optimal value for the dynamic strategy is found for low values of $|c_1|$ and $|c_2|$, where the imbalance price is approximately equal to the spot market price.

When relying on the static imbalance scenario, the economic revenues are maximized when λ^+ (c_1) is positive and λ^- (c_2) exceeds a value of approximately 40 €/MWh.

5. Discussion

Existing literature has paid limited attention to examining the value of solar power forecasting models, which can be effectively assessed by considering the economic error metric proposed in this study. In an earlier study [45], the authors suggest a *monotome* mapping of the quality and value, implying that a higher forecast quality corresponds to higher economic value. This is contradicted by the results presented in this study, as Section 4.4 shows that the economic value and accuracy are not linearly correlated. This is due to the dependence on the (real-time) market conditions and potential disruptions, which was also discussed in [15]. Technical error metrics are therefore not sufficient to address the economic value of forecasts. This study thus exposes the weakness of unidimensional model evaluation and identifies an added value of adopting economic metrics.

Firstly, economic metrics offer market participants that operate a PV plant valuable information on the most advantageous forecast model. The economic metric proposed in this study is capable of mapping the economic value of solar power forecasting modes by considering the market bidding process as well as the imbalance costs.

Secondly, the value of such economic metrics goes beyond market participants as the metrics provide insights into the ease of an electricity system to adequately manage the imbalance in real-time. The imbalance price is typically equal to the balancing energy price, which is set by the highest activated frequency restoration reserve bid on

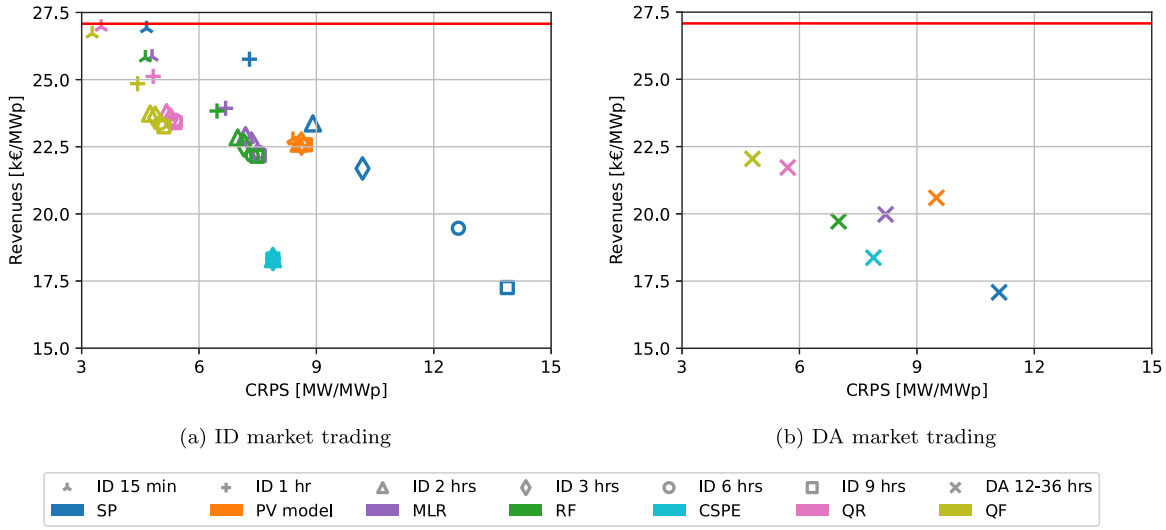

(a) ID market trading (b) DA market trading

Fig. 6. The economic revenue as a function of the CRPS. The red line indicates the revenues in case of perfect forecasting.

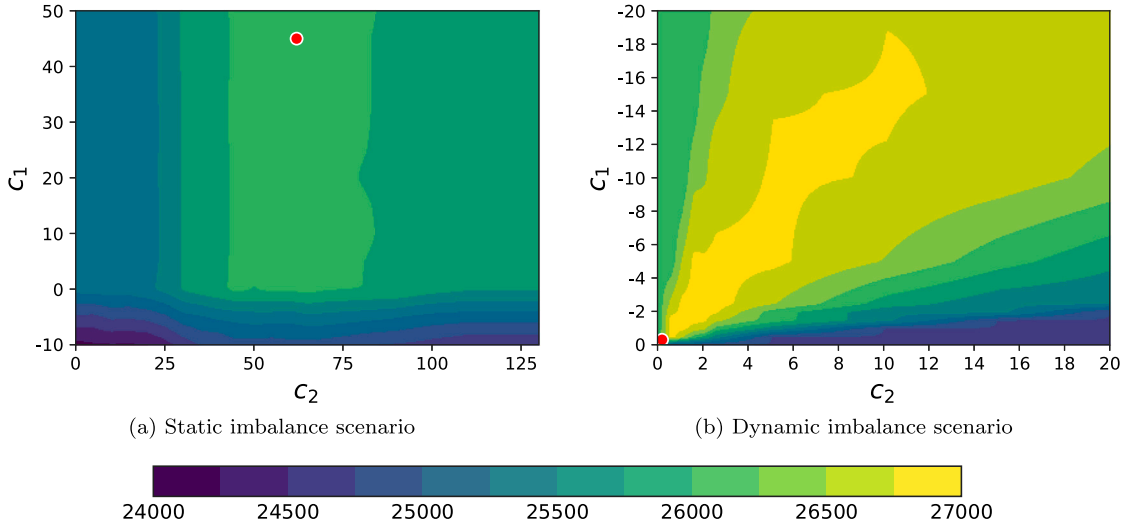

(a) Static imbalance scenario (b) Dynamic imbalance scenario

Fig. 7. Sensitivity analysis on the c_1 and c_2 value for the static and dynamic imbalance scenarios at $k = 1$. The color bar presents the obtained revenues in €/MWp, where the red dot indicates the optimal value.

the merit order list. A higher imbalance price therefore corresponds to times where expensive assets are deployed to restore the system's balance and thus indicate periods where the system's imbalance is large and/or available balancing capacity is limited. On the other hand, low imbalance prices typically indicate periods where there is an abundance of electricity, available balancing capacity and/or the system's imbalance is limited. In this regard, evaluating a solar power forecasting model on its economic value and in particular considering the imbalance costs, gives an (indirect) indication of its effect on the electricity system.

Therefore, it is recommended to utilize metrics that assess the economic value of solar power forecasting models. This economic evaluation not only provides insights into the expected economic revenues but also offers an indication of an electricity system's capability to manage imbalances. Looking forward, to expand the knowledge on the mapping between the technical and economic performance of solar power forecasting models, it is recommended to investigate the model performances on a multitude of locations that preferably feature varying market types that may require alternative economic metrics. Additionally, since the economic performance is driven by the market dynamics, it is suggested to closely inspect (extreme) events. These events encompass situations where e.g. the technical performance is above par, while the economic performance falls short and vice versa. Subsequently, a better understanding of the relation between the technical and economic performance is needed. This could also provide ground for improving the economic performance of solar power forecasting models, as it may assist in identifying periods with high and low economic risk.

6. Conclusion

This study proposes a novel operational multistage stochastic optimization model for market participants that operate a solar PV system. The method facilitates the generation of bids to the day-ahead and intraday market using probabilistic solar power forecasts. To achieve this, it employs a statistical scenario generation method that transforms probabilistic solar power forecasts into time-dependent scenarios. The results demonstrate the effectiveness of the stochastic bidding strategy and provide insights into the technical accuracy and economic value of various solar power forecasting models. The findings indicate that the proposed method outperforms the reference method, yielding higher revenues and causing less imbalance. This study also shows the value

of extending market participation from the day-ahead to the intraday market, resulting in a 22% increase in revenues and a halving of the total imbalance. Furthermore, the study explores the relationship between the accuracy of solar power forecasting models and their value, demonstrating that these are not linearly related.

CRediT authorship contribution statement

L.R. Visser: Writing – original draft, Visualization, Validation, Software, Methodology, Formal analysis, Data curation, Conceptualization. **T.A. AlSkaif:** Writing – review & editing, Methodology. **A. Khurram:** Writing – review & editing, Conceptualization. **J. Kleissl:** Writing – review & editing, Supervision. **W.G.H.J.M. van Sark:** Writing – review & editing, Supervision.

Declaration of competing interest

The authors declare that they have no known competing financial interests or personal relationships that could have appeared to influence the work reported in this paper.

Data availability

Data will be made available on request.

Acknowledgments

The authors would like to acknowledge the Hofvijverkring for their support through the fellowship grant. This work is part of the Energy Intranets (NEAT: ESI-BiDa 647.003.002) project, which is funded by the Dutch Research Council NWO, The Netherlands in the framework of the Energy Systems Integration & Big Data programme.

References

[1] IEA PVPS. Trends in photovoltaic applications 2023. Tech. rep, Paris; 2023, URL https://iea-pvps.org/wp-content/uploads/2023/04/IEA_PVPS_Snapshot_2023.pdf.
[2] Gandhi O, Kumar DS, Rodríguez-Gallegos CD, Srinivasan D. Review of power system impacts at high PV penetration Part I: Factors limiting PV penetration. Sol Energy 2020;210:181–201.
[3] Breyer C, Bogdanov D, Gulagi A, Aghahosseini A, Barbosa LS, et al. On the role of solar photovoltaics in global energy transition scenarios. Prog Photovolt, Res Appl 2017;25(8):727–45.
[4] Raza MQ, Nadarajah M, Ekanayake C. On recent advances in PV output power forecast. Sol Energy 2016;136:125–44.
[5] Yang D, Wang W, Gueymard CA, Hong T, Kleissl J, et al. A review of solar forecasting, its dependence on atmospheric sciences and implications for grid integration: Towards carbon neutrality. Renew Sustain Energy Rev 2022;161:112348.
[6] Ahmed A, Khalid M. A review on the selected applications of forecasting models in renewable power systems. Renew Sustain Energy Rev 2019;100:9–21.
[7] Hong T, Pinson P, Wang Y, Weron R, Yang D, Zareipour H. Energy forecasting: A review and outlook. IEEE Open Access J Power Energy 2020;7:376–88.
[8] Li B, Zhang J. A review on the integration of probabilistic solar forecasting in power systems. Sol Energy 2020;210:68–86.
[9] El-Baz W, Seufzger M, Lutzenberger S, Tzscheutschler P, Wagner U. Impact of probabilistic small-scale photovoltaic generation forecast on energy management systems. Sol Energy 2018;165:136–46.
[10] Cordova S, Rudnick H, Lorca A, Martinez V. An efficient forecasting-optimization scheme for the intraday unit commitment process under significant wind and solar power. IEEE Trans Sustain Energy 2018;9(4):1899–909.
[11] Kakimoto M, Endoh Y, Shin H, Ikeda R, Kusaka H. Probabilistic solar irradiance forecasting by conditioning joint probability method and its application to electric power trading. IEEE Trans Sustain Energy 2018;10(2):983–93.
[12] Lauret P, David M, Pinson P. Verification of solar irradiance probabilistic forecasts. Sol Energy 2019;194:254–71.
[13] Wang Y, Millstein D, Mills AD, Jeong S, Ancell A. The cost of day-ahead solar forecasting errors in the United States. Sol Energy 2022;231:846–56.
[14] Luoma J, Mathiesen P, Kleissl J. Forecast value considering energy pricing in California. Appl Energy 2014;125:230–7.
[15] Antonanzas J, Pozo-Vázquez D, Fernandez-Jimenez LA, Martinez-de Pison F. The value of day-ahead forecasting for photovoltaics in the Spanish electricity market. Sol Energy 2017;158:140–6.
[16] Pierro M, De Felice M, Maggioni E, Moser D, Perotto A, Spada F, Cornaro C. Photovoltaic generation forecast for power transmission scheduling: A real case study. Sol Energy 2018;174:976–90.
[17] Visser L, AlSkaif T, van Sark W. Operational day-ahead solar power forecasting for aggregated PV systems with a varying spatial distribution. Renew Energy 2022;183:267–82.
[18] Bracale A, Carpinelli G, De Falco P, Rizzo R, Russo A. New advanced method and cost-based indices applied to probabilistic forecasting of photovoltaic generation. J Renew Sustain Energy 2016;8(2):023505.
[19] Birkeland D, AlSkaif T. Research areas and methods of interest in European intraday electricity market research—A systematic literature review. Sustain Energy Grids Netw 2024;101368. http://dx.doi.org/10.1016/j.segan.2024.101368.
[20] Shinde P, Hesamzadeh MR, Date P, Bunn DW. Optimal dispatch in a balancing market with intermittent renewable generation. IEEE Trans Power Syst 2020;36(2):865–78.
[21] Silva AR, Pousinho H, Estanqueiro A. A multistage stochastic approach for the optimal bidding of variable renewable energy in the day-ahead, intraday and balancing markets. Energy 2022;258:124856.
[22] EPEX SPOT. The European power exchange. 2022, URL https://www.epexspot.com/en.
[23] Ntomaris AV, Marneris IG, Biskas PN, Bakirtzis AG. Optimal participation of RES aggregators in electricity markets under main imbalance pricing schemes: Price taker and price maker approach. Electr Power Syst Res 2022;206:107786.
[24] Gougheri SS, Jahangir H, Golkar MA, Ahmadian A, Golkar MA. Optimal participation of a virtual power plant in electricity market considering renewable energy: A deep learning-based approach. Sustain Energy Grids Netw 2021;26:100448.
[25] Campos RA, Martins GL, Rüther R. Assessing the influence of solar forecast accuracy on the revenue optimization of photovoltaic+ battery power plants in day-ahead energy markets. J Energy Storage 2022;48:104093.
[26] Gonzalez-Garrido A, Saez-de Ibarra A, Gaztanaga H, Milo A, Eguia P. Annual optimized bidding and operation strategy in energy and secondary reserve markets for solar plants with storage systems. IEEE Trans Power Syst 2018;34(6):5115–24.
[27] Conte F, Massucco S, Saviozzi M, Silvestro F. A stochastic optimization method for planning and real-time control of integrated pv-storage systems: Design and experimental validation. IEEE Trans Sustain Energy 2017;9(3):1188–97.
[28] Saez-de Ibarra A, Herrera VI, Milo A, Gaztañaga H, Etxeberria-Otadui I, Bacha S, Padros A. Management strategy for market participation of photovoltaic power plants including storage systems. IEEE Trans Ind Appl 2016;52(5):4292–303.
[29] Carriere T, Vernay C, Pitaval S, Neirac F-P, Kariniotakis G. Strategies for combined operation of PV/storage systems integrated into electricity markets. IET Renew Power Gener 2020;14(1):71–9.
[30] David M, Boland J, Cirocco L, Lauret P, Voyant C. Value of deterministic day-ahead forecasts of PV generation in PV+ storage operation for the Australian electricity market. Sol Energy 2021;224:672–84.
[31] Renkema Y, Brinkel N, Alskaif T. Conformal prediction for stochastic decision-making of PV power in electricity markets. 2024, arXiv preprint arXiv:2403.20149.
[32] Lago J, Marcjasz G, De Schutter B, Weron R. Forecasting day-ahead electricity prices: A review of state-of-the-art algorithms, best practices and an open-access benchmark. Appl Energy 2021;293:116983.
[33] Visser L, AlSkaif T, Hu J, Louwen A, van Sark W. On the value of expert knowledge in estimation and forecasting of solar photovoltaic power generation. Sol Energy 2023;251:86–105.
[34] Pinson P, Madsen H, Nielsen HA, Papaefthymiou G, Klöckl B. From probabilistic forecasts to statistical scenarios of short-term wind power production. Wind Energy 2009;12(1):51–62.
[35] Van der Meer D, Wang GC, Munkhammar J. An alternative optimal strategy for stochastic model predictive control of a residential battery energy management system with solar photovoltaic. Appl Energy 2021;283:116289.
[36] Yang D, van der Meer D. Post-processing in solar forecasting: Ten overarching thinking tools. Renew Sustain Energy Rev 2021;140:110735.
[37] Bröcker J, Smith LA. Increasing the reliability of reliability diagrams. Weather Forecast 2007;22(3):651–61.
[38] Thorarinsdottir TL, Scheuerer M, Heinz C. Assessing the calibration of high-dimensional ensemble forecasts using rank histograms. J Comput Graph Stat 2016;25(1):105–22.
[39] Holmgren WF, Hansen CW, Mikofski MA. Pvlib python: A python package for modeling solar energy systems. J Open Source Softw 2018;3(29):884.
[40] KNMI. KNMI data platform. 2022, URL https://dataplatform.knmi.nl/dataset/cesar-surface-meteo-lc1-t10-v1-0.
[41] ECMWF. European Centre for Medium-range Weather Forecasts, ECMWF. 2020, URL https://www.ecmwf.int/en/forecasts/datasets/archive-datasets.
[42] ENTSO-E. European Network of Transmission System Operators for electricity, ENTSO-E. 2020, URL https://transparency.entsoe.eu/.

[43] Tijdink A, Hoffman M, Vrolijk R, Van Breukelen B. Annual market update 2021: Electricity market insights. Tech. rep, TenneT; 2022, URL https://tennet-drupal.s3.eu-central-1.amazonaws.com/default/2022-07/Annual_Market_Update_2021_0.pdf.

[44] TenneT. Settlement prices. 2020, URL https://www.tennet.org/english/operational_management/export_data.aspx?exporttype=Onbalansprijs.

[45] Yang D, Alessandrini S, Antonanzas J, Antonanzas-Torres F, Badescu V, Beyer HG, Blaga R, et al. Verification of deterministic solar forecasts. Sol Energy 2020;210:20–37.